Dynamic Contact Angles and Flow in Vicinity of Moving Contact Line

Yulii D. Shikhmurzaev
Institute of Mechanics, Moscow University, 119899 Moscow, Russia

A previously developed mathematical wetting model is generalized and applied to the following two closely related situations: the spreading of a liquid over a prewet solid surface and the receding contact-line motion with a microscopic residual film, remaining behind the contact line. An analytical expression for the velocity dependence of the dynamic contact angle is derived. Macroscopic characteristics (the dynamic contact angle and drag force) and the flow field corresponding to the spreading of a liquid over a wet solid surface differ considerably from those calculated for a dry surface. Under certain conditions the flow in the reference frame fixed with respect to the contact line has a region with closed streamlines. The region appears due to the flow-induced Marangoni effect, the reverse influence of the surface tension gradient along the liquid-solid interface caused by the flow on the flow, which gives rise to the gradient. The results are compared qualitatively with experimental data.

Introduction

Mathematical modeling of wetting-dewetting processes in the framework of conventional fluid mechanics encounters fundamental difficulties due to the nonintegrable shear-stress singularity at the moving contact line, and the inability to describe the velocity-dependence of the dynamic contact angle (see Dussan V., 1979, for review). Furthermore, the problem is how to take into account the solid surface state, in particular, a microscopic liquid film, which may be initially present ahead of the advancing contact line or appear behind the receding contact line. (We use the term "advancing contact line" in a situation where a liquid spreads over a solid surface displacing a gas. The "receding" contact line refers to the reverse process. In both cases, the dynamic contact angle is measured through the liquid.) This film is invisible to conventional fluid mechanics and can strongly influence the macroscopic behavior of the liquid in wetting-dewetting phenomena (Rillaerts and Joos, 1980; Ghannam and Esmail, 1992). In contrast to *macroscopic* films (Landau and Levich, 1942; Bretherton, 1961), *microscopic* films cannot be described by macroscopic hydrodynamic equations not only because of their negligible thickness compared with characteristic length scales of the bulk flow but also due to the fact that the film formation and properties are controlled by the long-range intermolecular forces (Teletzke et al., 1988), which are not taken into account in conventional macroscopic hydrodynamics.

We may distinguish two possible methods of incorporating microscopic films in the modeling of wetting phenomena. The first is to consider the film as a layer of a finite thickness and take into account the factors, which become important on such small length scales, in particular, the factor of including the forces of nonhydrodynamic origin in the equations for the bulk flow (see de Gennes, 1985, for review). However, from this point of view, the "contact line," which is the region of interest in the wetting studies, will be located at the edge of the film.

The second method is to consider the flow on macroscopic length scales and take into account the presence of the microscopic film in the boundary conditions for the bulk flow. The idea to use the microscopic film as a remedy for the shear-stress singularity in the boundary conditions was mentioned in Dussan V. (1979), but no steps in this direction have been taken up to present. The influence of the microscopic films on the macroscopic characteristics of the flow and, in particular, on the dynamic contact-angle behavior was investigated experimentally, but no systematic theoretical studies of this problem have been reported.

The present study is carried out in the framework of an approach to the moving contact line problem initially formulated in Shikhmurzaev (1991). A mathematical model based on this approach (Shikhmurzaev, 1993a, 1994) eliminates the singularities inherent in the conventional approach of fluid

mechanics and allows describing the advancing liquid motion over a dry smooth solid surface in qualitative and quantitative agreement with experimental observations. The physical idea, which is the basis of the model, makes it possible to incorporate the microscopic film in the boundary conditions in a natural self-consistent way not as a remedy for the singularities but as a physical factor affecting the flow.

The modeling follows the results of experiments (Dussan V., 1979) which dictate that the advancing liquid motion is *rolling* (a liquid particle, which initially belongs to the free surface, traverses the three-phase interaction region in a finite time) and takes into account that an element of the gas-liquid interface does not change its properties instantly as it comes into contact with the solid wall: a certain relaxation period is required for this element to become an equilibrium element of the liquid-solid interface. The simplest mathematical model, which realizes this approach, predicts the appearance of the surface tension gradient along the liquid-solid interface, which influences the flow and, in particular, the dynamic contact angle and the force between the liquid and the solid in the vicinity of the moving contact line (Shikhmurzaev, 1993a, 1994). In the present work this approach is used to consider the receding contact-line problem with account of a microscopic residual film, remaining on the solid surface behind the contact line, and a closely related problem of the advancing contact-line motion across a prewet solid surface.

Background

Quantitative comparison of experimental data concerning the receding contact-line motion reported by different authors is difficult not only because dynamics of the receding interface was investigated not as systematically as wetting hydrodynamics, and very often experimental results correspond to different ranges of parameters, but also due to the appearance of the microscopic residual film, properties of which are controlled by poorly reproducible factors. Qualitative features of this phenomenon revealed by experimental studies may be summarized as follows:

(a) The receding liquid motion is *rolling* (Yarnold, 1938; Dussan V. and Davis, 1974), that is, material points initially located on the liquid-solid interface arrive at the moving contact line and then become elements of the gas-liquid interface in a finite time.

(b) The receding dynamic contact angle θ_d decreases as the contact-line speed U grows (Elliott and Riddiford, 1967; Johnson et al., 1977; Hopf and Stechemesser, 1988; Teletzke et al., 1988 and references therein).

(c) The maximum speed of the solid surface dewetting U_0 is finite, that is, a liquid displaced at a speed greater than U_0 is followed by a macroscopic liquid film remaining on the solid (Vaillant, 1913; see also Teletzke et al., 1988 for a review). In this case, the dynamic contact angle becomes equal to zero while the advancing contact angle at the same contact-line speed is far from its limiting value (Rose and Heins, 1962; Rillaerts and Joos, 1980; Hopf and Stechemesser, 1988; Sedev and Petrov, 1992). However, usually the degree of magnification in experimental studies is not reported, so that is difficult to conclude *what* contact angle (microscopic, macroscopic, or apparent) is measured.

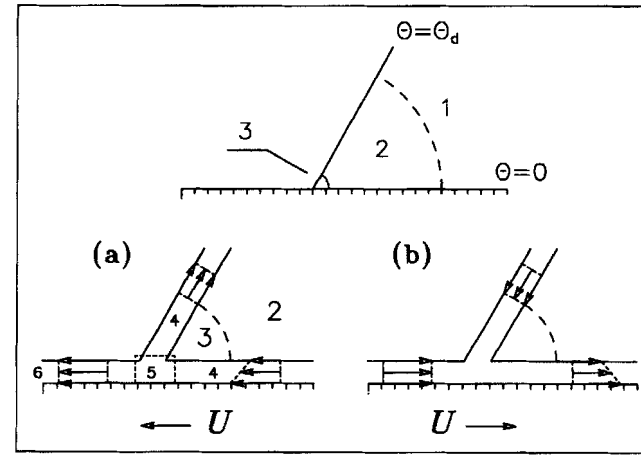

Figure 1. Flow in the interfaces in the immediate vicinity of the receding (a) and advancing (b) contact lines with account of a microscopic residual film.

For clearness the interfaces are depicted as layers of finite thickness. 1, 2, 3 correspond to the outer, intermediate, and inner asymptotic regions associated with characteristic length scales L, ϵL, and ϵCaL, respective; 4—interfaces, 5—three-phase interaction region ("contact line"), 6—microscopic residual film.

Since the receding contact line is usually followed by a microscopic film formed on the solid surface by adsorbed molecules of the liquid (Templeton, 1954, 1956), one should take into account that the rolling motion in this case implies that not all the molecules, which form a material point of the liquid-solid interface, arrive at the free surface: a part of them will be adsorbed by the solid surface (Figure 1). The dominating physical mechanisms of adsorption may be different for different liquid-solid systems (Fowkes, 1967), and they will not be considered here, since we are going to investigate only the influence of the integral properties of the microscopic film regardless of concrete physical mechanisms leading to its formation. Our interest will be focused on how the adsorbed microscopic film influences such characteristics of the three-phase interaction region as the mass and momentum balance at the contact line and what changes in the velocity-dependence of the dynamic contact angle and the drag force it will cause. Hereafter we will call "wet" the solid surface covered by the *microscopic* liquid film.

In itself the presence of the microscopic film (in contrast to the macroscopic one) does not remove the singularities of the classical formulation of the moving contact-line problem (Dussan V. and Davis, 1974) since it is invisible to macroscopic fluid dynamics and therefore does not change the shape of the domain where the macroscopic hydrodynamic equations are valid.

A microscopic residual film strongly influences hydrodynamics of a subsequent advancing contact-line motion (Rillaerts and Joos, 1980; Ghannam and Esmail, 1992). In experimental investigations of the advancing contact-line problem, some workers apply methods with many wetting-dewetting runs (Ablett, 1923; Wilkinson, 1975; Bolton and Middleman, 1980), and therefore the presence of the residual film becomes practically inevitable. Some of the others take special means to achieve thermodynamic equilibrium in a

gas/liquid/solid system (Elliott and Riddiford, 1967; Inverarity, 1969) and so the microscopic liquid film may appear, for example, due to the evaporation-condensation process. Convincing experimental data supporting this mechanism were recently reported by Novotny and Marmur (1991). In this connection, it is interesting to consider the influence of the microscopic residual film upon the main properties observed experimentally in the advancing contact-line motion and listed as (ii)–(iv) in the previous works of this series (Shikhmurzaev, 1991, 1993a, 1994):

(ii) Increase of the advancing dynamic contact angle as U grows

(iii) Existence of a maximum dynamic contact angle $\theta_{max} < 180°$ for some gas/liquid/solid systems

(iv) Existence of a maximum speed of wetting.

It is noteworthy that a precursor film preceding a slowly advancing "macroscopic" contact line in some gas/liquid/solid systems (Ausserré et al., 1986) in some cases can play the role of a microscopic residual film.

Theoretical investigations of different authors show that the flow in the bulk is independent of details of the flow in the immediate vicinity of the contact line (Dussan V., 1976; Hocking, 1977), and in many cases for the description of a wetting process only the macroscopic characteristics (such as the dynamic contact angle and the force between the liquid and the solid) are required. However, in a number of practical situations, the quality of films formed by solidified liquids depends on the flow structure in the vicinity of the moving contact line during the coating process. Since our model is able to describe the macroscopic characteristics of the advancing interface, it is reasonable to see what results it predicts for the flow structure. Therefore, the analysis of the flow field is one of the purposes of this article.

Thus, the scope of this article is twofold: (1) to investigate the influence of the microscopic film on the macroscopic characteristics, the dynamic contact angle and the force acting on the liquid in the vicinity of the moving contact line, of the advancing and receding fluid motions and (2) to analyze the flow field in the neighborhood of the moving contact line. In particular, we will derive a simple algebraic equation, which relates the dynamic contact angle with the contact-line speed and other parameters. We will also discuss a way of how to check the equation of state for the surface phase experimentally and obtain its parameters.

General Formulation

Let us recall the formulation of the moving contact-line problem in the framework of the model based on the true kinematics of the flow (Shikhmurzaev, 1993a, 1994). For the sake of simplicity, we assume that a displaced (or displacing) gas is inviscid and therefore dynamically passive. The Reynolds number of the flow is assumed to be small so that the inertial effects are negligible, and the flow in the bulk may be described by the Stokes equations.

The essence of the model (Shikhmurzaev, 1993a, 1994) is given by the boundary condition

$$\boldsymbol{n}\cdot\boldsymbol{P}\cdot(\boldsymbol{I}-\boldsymbol{nn})-\frac{1}{2}\nabla p^s=\beta(\boldsymbol{u}-\boldsymbol{U})\cdot(\boldsymbol{I}-\boldsymbol{nn}) \tag{1}$$

($\boldsymbol{I}$ is a metric tensor; $\boldsymbol{n}$ is a unit vector normal to the interface points from the solid to the liquid) and equations which describe distributions of the *surface* parameters along the liquid-solid interface

$$\frac{\partial\rho^s}{\partial t}+\nabla\cdot(\rho^s\boldsymbol{v}^s)=-\frac{\rho^s-\rho^s_{2e}}{\tau} \tag{2}$$

$$\boldsymbol{v}^s\cdot(\boldsymbol{I}-\boldsymbol{nn})=\frac{1}{2}(\boldsymbol{u}+\boldsymbol{U})\cdot(\boldsymbol{I}-\boldsymbol{nn})-\alpha\nabla p^s$$

$$(\boldsymbol{v}^s-\boldsymbol{U})\cdot\boldsymbol{n}=0 \tag{3}$$

$$p^s=\gamma(\rho^s-\rho^s_0) \tag{4}$$

completed by boundary conditions at and far from the contact line. Here $\boldsymbol{n}\cdot\boldsymbol{P}\cdot(\boldsymbol{I}-\boldsymbol{nn})$ is the shear stress acting on the interface ($\boldsymbol{P}$ is the stress tensor in the bulk); p^s is the *surface* pressure in the liquid-solid interface related with the *surface* density by the equation of state (Eq. 4), which is given in the simplest form applicable for isothermal and some barotropic processes in the surface phase; β is the coefficient of sliding friction (Bedeaux et al., 1976); $\boldsymbol{u}$ and $\boldsymbol{U}$ are the velocities of the liquid and the solid on the opposite sides of the liquid-solid interface. It is necessary to emphasize that p^s is not the surface tension of the solid; it is associated with the two-dimensional pressure in a thin layer of the liquid adjacent to the solid surface (Figure 1), and this quantity may be positive or negative (Gibbs, 1961). The righthand side of the surface mass balance equation (Eq. 2) describes the relaxation of the surface mass density due to the mass exchange between the interface and the bulk (ρ^s_{2e} and τ are the equilibrium surface density and the relaxation time, respectively). Obviously, this mass exchange may be neglected in the boundary conditions for the bulk velocity, and therefore on the interfaces one has

$$(\boldsymbol{u}-\boldsymbol{v}^s)\cdot\boldsymbol{n}=0. \tag{5}$$

Equations 3 relate the tangential components of the surface velocity $\boldsymbol{v}^s$ with the components of the bulk phase velocities on the opposite sides of the interface; α is a phenomenological coefficient describing in an integral form the influence of the surface pressure gradient on the velocity distribution across the interface.

Boundary conditions on the free surface derived in the same way as Eqs. 1–5 take the form (Shikhmurzaev, 1993a, 1994)

$$(\boldsymbol{u}-\boldsymbol{v}^s)\cdot\boldsymbol{n}=0$$

$$\boldsymbol{n}\cdot\boldsymbol{P}\cdot\boldsymbol{n}+p_g+p^s\kappa=0$$

$$(\boldsymbol{I}-\boldsymbol{nn})\cdot\boldsymbol{P}\cdot\boldsymbol{n}+\nabla p^s=0$$

$$\frac{\partial\rho^s}{\partial t}+\nabla\cdot(\rho^s\boldsymbol{v}^s)=-\frac{\rho^s-\rho^s_{1e}}{\tau}$$

$$(1+4\alpha\beta)\nabla p^s=4\beta(\boldsymbol{u}-\boldsymbol{v}^s)\cdot(\boldsymbol{I}-\boldsymbol{nn})$$

$$p^s=\gamma(\rho^s-\rho^s_0) \tag{6}$$

Here, p_g is the pressure in the gas; κ is the curvature of the free surface; ρ^s_{1e} is the equilibrium surface density in the liq-

uid-gas interface; the unit normal vector $\boldsymbol{n}$ points from the gas to the liquid. An extension of the model for the case of a liquid-liquid interface and a discussion on the physical meanings of parameters can be found elsewhere (Shikhmurzaev, 1993b).

In a stationary process, the total mass flux into and out of the moving contact line along the interfaces and the total force acting on the contact line are zero. These conditions, which link the distribution of the surface parameters along the liquid-gas and liquid-solid interfaces, together with some conditions for the overall flow give us the closed mathematical problem. In more details the mass and momentum balance conditions at the contact line will be discussed in the next section.

Let us briefly discuss the orders of magnitude of parameters involved in the model. All of the parameters have clear physical meanings, and since some of them will be the same for any mathematical model, which takes into account the interface formation process and dynamic properties of interfaces, their values have been already measured for some liquids. For example, the surface tension relaxation time τ can be measured by the oscillating jet method, and for water τ is about 10^{-3} s (see Kochurova et al., 1974 and references therein), although estimates give a smaller value. The coefficient of sliding friction β can be measured by considering flows through very thin capillaries (Churaev et al., 1984). Such experiments give for water $\beta \approx 3\times10^{4}$ N·s/m^3. The model derivation (Shikhmurzaev, 1993a) implies that β may be estimated as $\beta \sim \mu'/h$, where μ' is the viscosity in the interfacial layer and h is the layer thickness determined by intermolecular forces. Assuming that $\mu' \sim \mu$, we have that $h \sim 3\times10^{-8}$ m. This value slightly exceeds that predicted by the molecular theory of capillarity (Rowlinson and Widom, 1982). If the ordering of molecules in interfacial layers leads to $\mu' < \mu$, then the value of h must be reduced. This assumption agrees with the fact that β increases as temperature grows (Churaev et al., 1984). For the other parameters one has $\alpha \sim h/\mu'$, $\rho^s \sim \rho h$, $\gamma \sim (\partial p/\partial \rho)_T$ (Shikhmuraev, 1993a). Below, in the section dealing with the macroscopic characteristics of wetting, we will discuss a possibility of determining ρ_0^s and checking the surface equation of state by comparing theoretical results with experimental data. This would allow us to estimate h in an alternative way or, if β is also found, to obtain the viscosity in the interfacial layer μ', which could help to estimate other parameters.

The quanitative comparison of the model with experimental data is given in Shikhmurzaev (1993a), and different ways of the model generalization are discussed in Shikhmurzaev (1993a, 1994).

It is evident that boundary condition (Eq. 1), as well as an ordinary Navier slip model, eliminates the shear stress singularity inherent in the classical formulation, and Eqs. 1–6 give the usual boundary conditions for the Stokes equations far from the contact line, where the gradients of the surface parameters vanish. As shown in Shikhmurzaev (1993a), the first term on the lefthand side of Eq. 1 becomes important only in the immediate vicinity of the contact line, while in the major part of the slip region, slip is determined by the surface pressure gradient.

The time derivatives in Eqs. 2 and 6 vanish if we do not consider the unsteady process of the interface formation, which takes place, for example, if a liquid is instantaneously brought in contact with a solid. Otherwise, these derivatives must be held, and an initial distribution of the surface density or some other conditions regulating the evolution of the surface density must be set up.

Small Capillary Numbers and Relaxation Lengths

Let us consider the vicinity of a moving contact line with a characteristic length L small compared with that of the flow field and much greater than the characteristic thickness of liquid-gas and liquid-solid interfacial layers. For simplicity, we assume that the flow takes place in the plane perpendicular to the contact line and use a coordinate frame fixed with respect to it.

As has been shown in Shikhmurzaev (1993a, 1994) by applying the technique of matched asymptotic expansions to Eqs. 1–6 for small $\epsilon \equiv U\tau/L$ and capillary numbers, the free surface in the vicinity of the contact line is approximately planar, and one can distinguish the following three asymptotic regions (Figure 1):

(1) The outer region associated with the length scale L, which is far from the contact line and where the classical solution of the Stokes equations with the no-slip boundary condition on the solid surface and the zero tangential stress on a free surface is valid, and its inner limit is described by the following relationships (Moffatt, 1964):

$$u_{r(0)} = \frac{1}{r}\frac{\partial \psi_{(0)}}{\partial \theta}, \quad u_{\theta(0)} = -\frac{\partial \psi_{(0)}}{\partial r}, \tag{7}$$

$$\psi_{(0)} = \frac{rUu_w}{\sin\theta_d\cos\theta_d - \theta_d}[(\theta - \theta_d)\sin\theta - \theta\cos\theta_d\sin(\theta - \theta_d)]$$

(hereafter ϕ, $\boldsymbol{u}_r$ and $\boldsymbol{u}_\theta$ denote the stream function, the radial and transversal component of the velocity field in the bulk, respectively; (r, θ) are the plane polar coordinates with the contact line placed at the origin and the axis $\theta = 0$ parallel to the solid surface; θ_d, $\boldsymbol{U}$ are the dynamic contact angle and the absolute value of the speed of the solid wall; the parameter u_w is equal to 1 for the advancing contact line and -1 for receding; the subscript 0 in parentheses marks the velocity components of the classical solution).

(2) The "intermediate" region with characteristic dimensions of order $l = U\tau$, in which the properties of "surface phases" can considerably change, and the surface tension gradient along the liquid-solid interface, appears. This gradient causes the apparent slip on the liquid-facing side of the liquid-solid interface (see Figure 1). In this region the thickness of interfacial layers may be neglected and one may consider the interfaces as geometrical surfaces with zero thickness and specific "surface" properties (the surface tension, etc).

(3) The "inner" (or "viscous") region with dimensions of order Cal ($Ca = \mu U/\sigma \ll 1$ is the capillary number, μ denotes the viscosity of the liquid and σ is the surface tension at the free surface). This region includes the three-phase interaction zone (i.e., the "contact line"), parts of the interfaces and the adjacent liquid. In this region viscous stresses become comparable with the surface tension gradients. Obviously, if one deals with the flow associated with the characteristic length scale l and is interested in the main terms in

Ca as $Ca \to 0$, the dimensions of the "inner" region may be neglected.

The main terms in asymptotic expansions in Ca of θ_d and the force between the liquid and the solid as $Ca \to 0$ are determined by the solution in the "intermediate" region: the integral contribution of the inner region is of $O(Ca)$ and may be neglected in comparison with terms of order unity as $Ca \to 0$. It is very important to emphasize that within this accuracy the force between the liquid and the solid is determined by the surface tension gradient along the liquid-solid interface in the "intermediate" region and not by the shear stress: an element of the liquid-solid interface with a negligible mass experiences the action of three forces, namely, (1) the shear stress, (2) the surface tension gradient, (3) the drag force from the solid, and the first force (of order $\mu U/l$) may be neglected compared with the second one (which is of order σ/l) as $Ca \to 0$.

It is necessary to remember that for applicability of the theory, l must be large compared with a characteristic interfacial layer thickness h determined by intermolecular forces in contacting media. If $l \sim h$, the physical background of the theory remains of course valid, though in this case, the order-of-magnitude analysis of the model's parameters, which was discussed above, is not applicable, and one has to use them as empirical constants while comparing the theory with experimental data. At the same time, it should be pointed out that as demonstrated in Shikhmurzaev (1994) $l \equiv U\tau$ is the low limit of the actual relaxation length as the contact line speed tends to infinity.

Let us develop the approach briefly described above to consider the solution in the intermediate region for the advancing and receding contact line motions in the case where a microscopic residual film formed by adsorbed molecules of the liquid is present (or appears) on the solid surface.

First of all, we must clarify the following aspects of our analysis in order to avoid possible misunderstanding:

(1) Since we consider the flow on a length scale large compared with the thickness of the interfacial layers and that of the microscopic film, the latter may be regarded a 2-D fluid, which properties may be described by some integral characteristics resulting from the averaging across the film of the distribution of the actual parameters. Thus, we will not consider the microscopic film structure, which depends on the long-range forces leading to the appearance of this film (de Gennes, 1985).

(2) The existence of the *microscopic* film ahead or behind the film does not mean that the contact line is removed, and hence the singularities disappear. Indeed, in contrast to *macroscopic* liquid films (Landau and Levich, 1942; Bretherton, 1961), the bulk hydrodynamic equations, which do not include long-range intermolecular forces, are inapplicable to describe the *microscopic* film. Thus, the flow domain, where our bulk equations are valid and on which boundaries the boundary conditions must be formulated, remains the same if the microscopic film is present or not, and the line formed at the intersection of the two surfaces of the flow domain boundary is called the contact line. The fact that a precursor (microscopic) film may alter only the boundary conditions but not the flow domain shape, if the flow on a macroscopic length scale is considered, was mentioned also in Dussan V. (1979).

The closed formulation of the problem in the intermediate region can be obtained by applying the asymptotic technique to the general problem, which includes the Stokes equations in the bulk, the conditions (Eqs. 1–6) on liquid-solid and liquid-gas interfaces and the surface mass and momentum balance equations at the contact line (Shikhmurzaev, 1993a, 1994). The main terms in Ca and ϵ of the velocity and pressure in the intermediate region obey the Stokes equations

$$\nabla \cdot \boldsymbol{u} = 0, \quad \nabla p = \Delta \boldsymbol{u} \tag{8}$$

with boundary conditions on the free surface

$$u_r(r, \theta_d) = u_{r(0)}(\theta_d; u_w), \quad u_\theta(r, \theta_d) = 0$$

$$u_{r(0)}(\theta_d; u_w) = u_w \frac{\sin\theta_d - \theta_d \cos\theta_d}{\sin\theta_d \cos\theta_d - \theta_d} \tag{9}$$

and the velocity on the liquid-facing side of the liquid-solid interface, which is related with the surface velocity v_2^s and pressure p_2^s, of the liquid-solid interface by

$$u_r(r,0) = 2v_2^s - u_w + \frac{2A}{(1+4A)V^2}\frac{dp_2^s}{dr}, \quad u_\theta(r,0) = 0 \tag{10}$$

Hereafter we use the variables made dimensionless by the scaling quantities $l = U\tau$, U, $\mu U/l$ and σ. The subscripts 1 and 2 mark the surface parameters of the gas-liquid and liquid-solid interfaces, respectively; the parameter

$$V = U\sqrt{\frac{(1-\rho_{1e}^s)\tau\beta}{\sigma(1+4A)}}$$

will be called the dimensionless contact-line speed; the subscript e marks the equilibrium values of corresponding surface parameters; $A = \alpha\beta$ characterizes the influence of the surface pressure on the relationship between the velocity difference across the interface and the surface velocity; the surface densities are made dimensionless using ρ_0^s, that is, the surface density corresponding to the zero surface tension (see Eq. 4).

Distributions of the surface parameters along the liquid-solid interface are described by the set of equations

$$\frac{d\rho_2^s v_2^s}{dr} = -(\rho_2^s - \rho_{2e}^s), \quad \frac{d\rho_2^s}{dr} = 4V^2(u_w - v_2^s) \tag{11}$$

with boundary conditions

$$\rho_2^s(0)v_2^s(0) = -\rho_{1e}^s u_{r(0)}(\theta_d; u_w) + \rho_{\text{res}}^s u_w \tag{12}$$

$$\cos\theta_d = \frac{\rho_2^s(0) - 1}{1 - \rho_{1e}^s} - p_{\text{res}}^s \tag{13}$$

$$\rho_2^s \to \rho_{2e}^s, \quad v_2^s \to u_w \quad \text{as} \quad r \to \infty \tag{14}$$

$$p^s = \lambda(\rho^s - 1), \quad \lambda = 1/(1 - \rho_{1e}^s) \tag{15}$$

Here Eqs. 12 and 13 (the latter is simply the Young equation written down in our notations) describe the balance of mass

and momentum at the contact line; Eqs. 14 match the solutions in the intermediate and outer regions; the equation of state (Eq. 15) connects the (dimensionless) surface pressure, which is defined as minus surface tension, with the (dimensionless) surface density. In statics, the usual Young equation relates the equilibrium surface densities ρ^s_{1e}, ρ^s_{2e} and the static contact angle θ_0:

$$\rho^s_{2e} = 1 + (1 - \rho^s_{1e})(\cos\theta_0 + p^s_{\text{res}}) \tag{16}$$

The presence of the microscopic film on the solid surface is manifested by:

- An additional mass flux into (or out of) the contact-line region (the last term in Eq. 12, where ρ^s_{res} is the surface density of the film);
- An alteration of the force acting on the contact line (see Eqs. 13 and 16, where p^s_{res} generally is not equal to p^s_{SG}, the tangential force per unit length acting on the contact line in the absence of the residual film).

Since generally $p^s_{\text{res}} \neq p^s_{SG}$, the static contact angle on the dry surface θ_s usually differs from the static contact angle on a wet surface θ_0: these quantities are related by

$$\cos\theta_s + p^s_{SG} = \cos\theta_0 + p^s_{\text{res}} \tag{17}$$

The surface density of the residual film ρ^s_{res} should be related with p^s_{res} by an equation of state, which is determined by the properties of contacting media. In the receding contact-line motion ρ^s_{res} (and, consequently, p^s_{res}) is also a function of the distance from the contact line due to some relaxation process of the residual film formation. Its value at $r = 0$ used in Eq. 12 depends also on the conditions of the residual film formation, i.e., on the dimensionless contact line speed V. Obviously, $p^s_{\text{res}} \to p^s_{SG}$ as $\rho^s_{\text{res}} \to 0$.

First, we will analyze the influence of ρ^s_{res} and p^s_{res} on the contact-line motion separately by considering them as independent *constants*. This is a reasonable assumption for the advancing liquid flow and under certain conditions may be a good approximation for the receding one. Then we will consider what qualitative changes in the dynamic contact-angle behavior will appear if ρ^s_{res} is velocity-dependent. A general question concerning the relationship $p^s_{\text{res}} = f(\rho^s_{\text{res}})$ will remain opened for a discussion and experimental investigation.

The model (Eqs. 11–17) has an interesting consequence. According to the present view of the situation, the static contact-angle hysteresis is caused by the heterogeneity of the solid surface due either to chemical contamination (Joanny and de Gennes, 1984; Pomeau and Vannimenus, 1985) or to surface roughness (Oliver and Mason, 1977; Dussan V., 1979; Cox, 1983). Figure 2 illustrates a possibility of the contact-angle hysteresis on a *smooth homogeneous* solid surface: a droplet forced to spread tends to restore its shape and gives rise to a residual film, which changes the static contact angle according to Eq. 17. As will be discussed below, the residual film properties may be dependent on the contact line speed, and therefore the stationary shape of a droplet on a smooth solid surface will depend on the history of its deformation. Thus, a family of equilibrium shapes of the droplet on a smooth homogeneous solid surface is possible. Certainly, in reality all the factors leading to the contact angle hysteresis (surface roughness, chemical inhomogeneities of the solid surface, the residual film appearance) take place. It should be pointed out also that the mechanism of the contact angle hysteresis described here differs from that of a pseudo-hysteresis due to a quasi-static motion of the receding contact line (Hansen and Miotto, 1957).

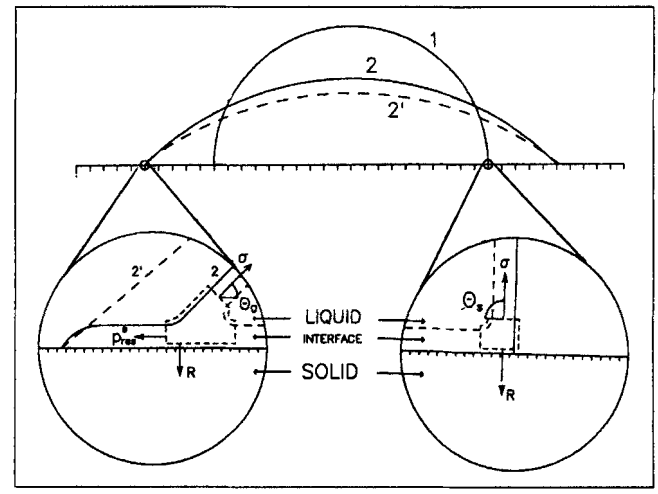

Figure 2. Static contact-angle hysteresis on a smooth homogeneous solid surface.

A drop forced to spread from 1 to 2′ tends to restore its shape and leaves a microscopic residual film formed by adsorbed molecules on the solid surface. This film alters the tangential force acting on the contact-line region and therefore changes the static contact angle.

Of course, considering the influence of the receding liquid on the condition of the solid surface is not a novel idea (see, for example, Bartell and Wooley, 1933). However, in previous works, it was assumed that the receding liquid alters the solid surface structure and therefore changes the surface tension of a gas-solid interface, that is, the force acting on the contact line. In the present model we consider not only the changes of the force acting on the contact line due to the microscopic residual film appearance in the receding contact line motion, but also the microscopic mass flux out of the contact line region. In statics, both statements are equivalent (since in statics, there are no mass fluxes), but as will be shown below, in dynamics, the mass flux out of the three-phase interaction region plays a much more important role than the changes in the tangential force density.

Analytical Results

Although the numerical analysis of the problem (Eqs. 11–16) is rather simple, it is necessary to remember that the moving contact line problem is only an ingredient of many more complex problems, and, therefore, a simple way of obtaining the parameters important for a global problem is desirable. In the present section we consider simplifications which are possible in the case of low-compressible liquids. As has been shown in Shikhmurzaev (1993a), in this case $\lambda^{-1} \equiv (1 - \rho^s_{1e}) \ll 1$. This fact has not been taken into account before, and now we will apply the usual perturbation technique to the problem (Eqs. 11–16) using the limit $\lambda^{-1} \to 0$.

Expanding all the unknown functions in power series of λ^{-1} and exploiting the regular procedure of the perturbation

technique, we obtain from Eqs. 11–16 the following expressions valid to the terms of the first order in λ^{-1}

$$\rho_2^s = \rho_{2e}^s + C\lambda^{-1}\exp(-kr)$$
$$v_2^s = u_w + \frac{Ck}{4\lambda V^2}\exp(-kr) \quad (18)$$

$$u_r(r,0) = u_w + \frac{Ck}{2\lambda V^2(1+4A)}\exp(-kr)$$
$$k = \frac{2V}{\rho_{2e}^s}\left(\sqrt{V^2+\rho_{2e}^s} - u_w V\right) \approx 2V\left(\sqrt{V^2+1} - u_w V\right) \quad (19)$$

Mass and momentum balance Eqs. 12 and 13 give two expressions for the unknown constant of integration C. Eliminating C from these expressions, we get the following algebraic equation which relates the dynamic contact angle value θ_d with other parameters:

$$(\cos\theta_0 - \cos\theta_d)\left[1 + \frac{\sqrt{V^2+1} - u_w V}{2u_w V}\right]$$
$$= \frac{1+\rho_{1e}^s u_w^{-1} u_{r(0)}(\theta_d, u_w) - \rho_{\text{res}}^s}{1-\rho_{1e}^s} + \cos\theta_0 + p_{\text{res}}^s \quad (20)$$

Equation 20 gives an excellent approximation of the numerically obtained velocity dependence of θ_d for $\lambda \geq 10$. For C one has $C = \cos\theta_d - \cos\theta_0$ and, obviously, $Cu_w \leq 0$.

Equation 20 generalizes the corresponding relationship obtained in Shikhmurzaev (1994) and includes some of empirical relationships known in literature as particular cases.

The fluid velocity distribution along the liquid-solid interface given by Eq. 10 has an interesting property. If

$$D = -\frac{Ck}{2u_w\lambda V^2(1+4A)} > 1 \quad (21)$$

then there is a stagnation point located at the distance

$$r_0 = k^{-1}\ln D \quad (22)$$

from the origin so that $u_r(r,0)u_w < 0$ if $r < r_0$, and $u_r(r,0)u_w > 0$ if $r > r_0$. As will be shown below, the condition (Eq. 21) corresponds to appearance of the region with closed streamlines near the contact line.

Macroscopic Characteristics

Problem 11–16 can be solved independently of the flow field consideration. Its solution gives the dynamic contact-angle value θ_d, and the tangential force exerted on the liquid by the solid in the vicinity of the contact line. This (total) force is equal to the integral of the surface pressure gradient along the liquid-solid interface and can be expressed as (Shikhmurzaev, 1993a, 1994)

$$F = p^s(\rho_{2e}^s) - p^s(\rho_2^s(0)) \quad (23)$$

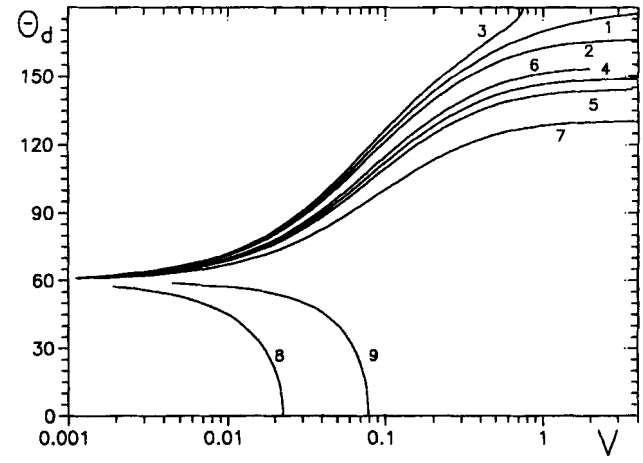

Figure 3. Advancing dynamic contact angle vs. dimensionless contact-line speed.

Curves 1–3 correspond to a dry solid surface ($\rho_{\text{res}}^s = 0$) and $\rho_{1e}^s = 0.95$, $\theta_s = 60°$: 1— $p_{\text{SG}}^s = 0$; 2— $p_{\text{SG}}^s = -0.5$; 3— $p_{\text{SG}}^s = 0.5$. Curves 4–7 were obtained for a wet surface and $\rho_{1e}^s = 0.95$, $\theta_0 = 60°$: 4— $\rho_{\text{res}}^s = 0.1$, $p_{\text{res}}^s = 0$; 5— $\rho_{\text{res}}^s = 0.1$, $p_{\text{res}}^s = -0.5$; 6— $\rho_{\text{res}}^s = 0.1$, $p_{\text{res}}^s = 0.5$; 7— $\rho_{\text{res}}^s = 0.2$, $p_{\text{res}}^s = 0$. Curves 8 and 9 describe the velocity-dependence of the receding contact angle for $\rho_{1e}^s = 0.95$: 8— $\rho_{\text{res}}^s = 0$, $p_{\text{SG}}^s = 0$, $\theta_s = 60°$; 9— $\rho_{\text{res}}^s = 0.4$, $p_{\text{res}}^s = 0$, $\theta_0 = 60°$.

Combining Eqs. 13, 15, 16, and 23, we obtain

$$F = \cos\theta_0 - \cos\theta_d(V) \quad (24)$$

It is easy to show that Eq. 24 remains valid if Eq. 15 is replaced by an arbitrary equation of state: Eq. 24 is a direct consequence of Eq. 23 and the Young equations for static and dynamic situations. In the receding contact line motion if ρ_{res}^s depends on V, the contact angle θ_0 also becomes velocity-dependent, but Eq. 24 remains still valid.

Figure 3 shows the numerically obtained dependences of the advancing contact angle θ_d on V for dry (curves 1–3) and wet (4–7) solid surfaces; curves 8 and 9 correspond to a receding contact line and will be discussed later.

In the case of a dry solid surface, the value and the sign of p_{SG}^s qualitatively influence the flow characteristics. If $p_{\text{SG}}^s > 0$, the system has a maximum speed of wetting V_*: if $V > V_*$, then the solution of Eqs. 11–16 fails to exist. This fact was interpreted as the transition from the rectilinear contact line to a "sawtooth" one (Shikhmurzaev, 1993a). Experimentally, the existence of a maximum speed of wetting was demonstrated by Blake and Ruschak (1979). If $p_{\text{SG}}^s < 0$, then θ_d asymptoties to a certain value $\theta_{\max} < 180°$ as V increases. However, for reasonable values of p_{SG}^s the deviation of θ_d from 180° is relatively small (Shikhmurzaev, 1993a, 1994) though in experiments (Elliott and Riddiford, 1967; Inverarity, 1969) for some systems $\theta_{\max} = 115°$. Thus, it is interesting to see if variations of any other parameter can lead to $\theta_{\max}$ considerably less than 180°.

In Figure 3, it is shown that even a very thin microscopic film ($\rho_{\text{res}}^s = 0.1$) strongly decreases θ_d even for positive p_{res}^s. In complete agreement with experimental observations, the dynamic advancing contact angle associated with the flow over a pre-wet solid surface is lower than that obtained for the dry solid surface (Rillaerts and Joos, 1980; Ghannam and Esmail,

1992), and, if the static contact angle in both cases is the same (Rillaerts and Joos, 1980), θ_d increases not so rapidly in the case of a prewet solid surface as it does if the surface is dry.

It is interesting to mention the following fact. Many experimenters reported that in their studies the dynamic contact angles of values very close to 180° were not observed. For example, Ghannam and Esmail (1992) demonstrated that for their roll-coating systems they were not able to record stable contact angles higher than 160°. Slight unsteady movement by the dynamic contact line was observed at higher substrate speeds, followed by the onset of an air entrainment by the coating liquid. This implies that in the considered case, the air entrainment is due to hydrodynamic instability and not to the passing over the maximum speed of wetting.

Quantitative comparison with the above cited experiments is difficult due to the lack of information about some parameters involved in the theory. It is also necessary to remember that, strictly speaking, the theory is applicable if $l \gg h$, i.e., not for the case of very small speeds of wetting.

Figure 3 illustrates mainly the influence of ρ^s_{res} for the situation when the static contact angle is the same for different systems; the changes in the static contact angle due to the presence of the microscopic film with $p^s_{\text{res}} \neq 0$ are described by Eq. 17.

In the advancing contact-line motion, the value of ρ^s_{res} may be considered as independent of V: it is determined by the properties of contacting media and by the conditions at which the film was formed, i.e., on the history of wetting.

Surface equation of state

The above-described behavior of θ_d for a liquid spreading over a prewet solid surface suggests a way of experimental checking the surface equation of state (Eq. 4) and determining its parameters. Experiments (see, for example, Rillaerts and Joos, 1980) show that wetting hydrodynamics strongly depends on the presence of a microscopic liquid film on the solid surface ahead of the spreading liquid, and this fact supports our assumption that p^s may be considered as a function of ρ^s. The problem is how to organize experiments and combine the results with the theoretical predictions in order to obtain this function.

As is clear from Figure 3, the (dimensionless) surface density of the microscopic film strongly influences (a) the rate of growth of the dynamic contact angle and (b) its limiting value at high contact line speed. Thus, if we know the (dimensional) surface film density ρ^s_{res}, for example, by controlling the evaporation-condensation process, which gives rise to its appearance, and are able to measure the velocity-dependence of θ_d (or at least $\theta_{\max}$), then we can use ρ^s_0, which was taken to be a scale for making ρ^s_{res} nondimensional, as an adjustable parameter trying to fit the theory to experimental data. The obtained value of ρ^s_0 would allow us to estimate the interfacial layer thickness h ($\rho^s_0 \sim \rho h$), which could then help to calculate other parameters. If we are able to *vary* ρ^s_{res} and measure a *function* $\theta_{\max}$ (ρ^s_{res}), then we could determine the whole functional dependence $p^s(\rho^s)$, which should replace the simplest linear surface equation of state (Eq. 4) used in this article. We remind the reader that p^s_{res} or, more precisely, the difference $p^s_{\text{res}} - p^s_{\text{SG}}$ can be measured in statics (see Eq. 17). Experiments with liquids spreading over prewet solid surfaces could also allow us to investigate, at first, qualitatively, the influence of other possible arguments in the surface equation of state, such as the parameters characterizing electrohydrodynamic properties of contacting materials, since one can prepare and influence the film ahead of the contact line without changing the properties of the spreading liquid.

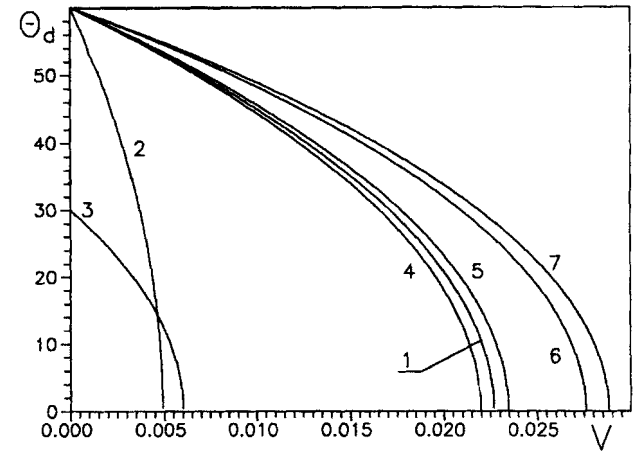

Figure 4. Receding dynamic contact angle vs. contact-line speed for $\rho^s_{\text{res}} = \text{const}$.

Curve 1 is obtained for $\rho^s_{1e} = 0.95$, $\rho^s_{\text{res}} = 0$, $p^s_{\text{res}}(= p^s_{\text{SG}}) = 0$, $\theta_0(= \theta_s) = 60°$. The parameters of the others differ as follows: 2— $\rho^s_{1e} = 0.99$; 3— $\theta_0 = 30°$; 4— $p^s_{\text{res}} = 0.5$; 5— $p^s_{\text{res}} = -0.5$; 6— $\rho^s_{\text{res}} = 0.1$; 7— $\rho^s_{\text{res}} = 0.1$, $p^s_{\text{res}} = -0.5$.

Receding contact lines

In the receding contact line motion generally $\rho^s_{\text{res}} = \rho^s_{\text{res}}(V)$. In Figure 4, we have shown the receding contact angle vs. V for a particular case $\rho^s_{\text{res}} = \text{const}$, that is, in the situation where the dependence of ρ^s_{res} upon V may be neglected. The value of θ_d decreases as V grows and becomes zero at a finite $V = V_0$. The value of V_0 strongly depends on ρ^s_{1e}, θ_0, and ρ^s_{res} being practically independent of p^s_{res}. Qualitative behavior of experimental curves is similar. If $V > V_0$, the solution of Eqs. 11–16 fails to exist. It means that the *macroscopic* film is pulled out of the receding liquid. Obviously, this film may be described by the bulk hydrodynamic equations. The edge of this macroscopic film is the actual contact line, and it moves at the speed equal to V_0, while the rest of the liquid may be displaced at a speed greater than V_0, thus increasing the length of the macroscopic film.

It is noteworthy that the receding dynamic contact angle changes from θ_0 to zero as V increases not for an arbitrary dependence $\rho^s_{\text{res}}(V)$: an analysis of the problem (Eqs. 11–16) shows that the (dimensionless) mass flux into the (receding) contact line from the liquid-solid interface (in a coordinate frame fixed with respect to the contact line) decreases as V increases, and therefore the mass flux out of the contact line region due to the residual film motion is bounded. It means that ρ^s_{res} and V_0 are bounded as well.

At $V = V_0$ the corresponding advancing dynamic contact angle is far from its maximum value (see curves 8 and 9 in Figure 3).

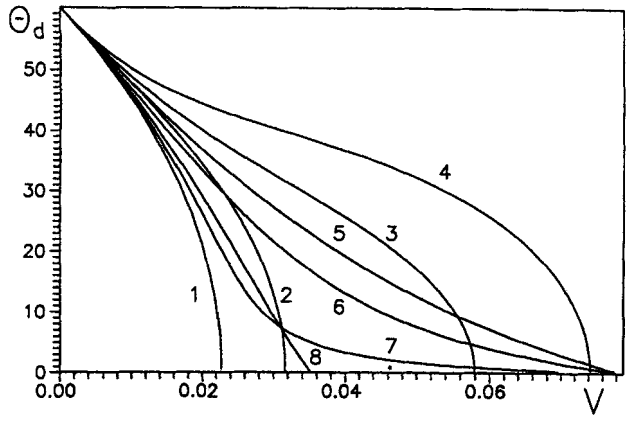

Figure 5. Velocity-dependence of the receding dynamic contact angle for a velocity-dependent residual film density.

Curves 1-4 correspond to Eq. 25: 1— $\rho_r^s = 0$; 2— $\rho_r^s = 0.2$, $W = 2$; 3— $\rho_r^s = 0.4$, $W = 2$; 4— $\rho_r^s = 0.4$, $W = 3$. Curves 5-8 were obtained using Eq. 26: 5— $\rho_r^s = 0.4$, $b = 0$; 6— $\rho_r^s = 0.4$, $b = 1$; 7— $\rho_r^s = 0.4$, $b = 10$; 8— $\rho_r^s = 0.2$, $b = 1$.

For an arbitrary function $\rho_{res}^s(V)$, the maximum speed of dewetting V_0, that is, the maximum value of V for which a solution of Eqs. 11-16 exists, corresponds in a general case to a nonzero value of the dynamic contact angle.

In a general case, the function $\rho_{res}^s(V)$ can be found either experimentally or theoretically by considering kinetics of the microscopic residual film formation (see Teletzke et al., 1988 and references therein). Here we will consider two possible examples of such a dependence. Curves 1-4 in Figure 5 correspond to the simplest relationship

$$\rho_{res}^s(V) = \rho_r^s[1 - \exp(-V/W)] \tag{25}$$

and curves 5-8 are obtained using the function

$$\rho_{res}^s(V) = \rho_r^s \frac{1 - \theta_d(V)/\theta_0}{1 + b\theta_d(V)/\theta_0}, \tag{26}$$

which connects ρ_{res}^s and V in an implicit way through the velocity-dependence of θ_d (ρ_r^s, W, b are empirical constants). It is evident that Eq. 25 includes $\rho_{res}^s = \text{const}$ as a particular case ($W = 0$), and for both Eqs. 25 and 26 ρ_r^s is the upper limit of ρ_{res}^s. For simplicity, we assume that $p_{res}^s \equiv 0$. Qualitative behavior of curves 1-4 is close to that obtained for constant values of ρ_{res}^s, while the shapes of curves 5-8 are completely different.

Experimental data reported in the literature have the same qualitative behavior as the theoretical curves described by Eq. 25. Unfortunately, the lack of information about some parameters of the model does not allow us to compare the theory with experiments quantitatively.

Thus, we may state that a function $\rho_{res}^s(V)$ strongly influences the receding dynamic contact angle behavior, and a function $\theta_d(V)$ obtained experimentally could be used, at least in principle, for receiving information about the residual film formation. For example, resolving Eq. 20 for ρ_{res}^s and using the independently measured values of other parameters, one could calculate the function $\rho_{res}^s(V)$, which then can give useful information for structural theories. A qualitative analysis of the data reported by Hopf and Stechemesser (1988) and Sedev and Petrov (1992) shows that the residual film density increases tending to a certain limiting value as the contact line speed grows.

The present model, which predicts a finite speed of dewetting even in the case of a velocity-dependent residual film density, eliminates the apparent contradiction, pointed out by Blake (1993), between the progressive thickening of the entrained *microscopic* film (Teletzke, 1983) and the abrupt onset of the *macroscopic* film entrainment.

Flow Field

A solution of the problem (Eqs. 11-16) gives

- The value of θ_d, which determines the flow domain and the velocity of the liquid on the gas-liquid interface (see Eqs. 13 and 9);
- The surface parameters distribution along the liquid-solid interfacial layer and, in particular, the velocity of the liquid on the liquid-solid interface (see Eq. 10).

It is convenient to rewrite Eqs. 8-16 as a problem for the stream function ψ in a wedge region $\{r, \theta | r \geq 0,\ 0 \leq \theta \leq \theta_d\}$ as follows:

$$\Delta^2\psi = 0$$

$$\psi = 0, \quad \frac{1}{r}\frac{\partial\psi}{\partial\theta} = u_{r(0)}(\theta_d; u_w) \quad \text{for} \quad r > 0, \theta = \theta_d$$

$$\psi = 0, \quad \frac{1}{r}\frac{\partial\psi}{\partial\theta} = u_r(r,0) \quad \text{for} \quad r > 0, \theta = 0 \tag{27}$$

Here $u_{r(0)}(\theta_d; u_w)$ is determined by Eq. 9, and $u_r(r,0)$ is related with the solution of Eqs. 11-16 by Eq. 10 or Eq. 19. The force experienced by the liquid is given by Eq. 24. The Mellin transform allows us to reduce the problem (Eq. 27) to a standard boundary-value problem for a linear ordinary differential equation of the 4th order with constant coefficients, which can be easily solved analytically. After overcoming usual difficulties inherent in the numerical inverse Mellin transform (Davies and Martin, 1979), we obtain the velocity components and are able to draw streamlines.

Calculations show that gradients of the surface quantities increase as $r \to 0$ along the liquid-solid interface. For qualitative description of the flow-field evolution it is convenient to use the function D, which was introduced above. If $D < 1$, then slip at the origin is partial, $[u_w - u_r(r,0)]/u_w < 1$; $D > 1$ means that the so-called *reverse* slip takes place, $[u_w - u_r(r,0)]/u_w > 1$. The case $D = 1$ corresponds to complete slip at the origin, $u_r(r,0) \to 0$ as $r \to 0$. It is necessary to remind that we are dealing only with parameters of the intermediate region, and here the origin means the vicinity of the inner region, where the influence of bulk stresses on the surface parameters distribution is important, and the surface and bulk problems become interrelated.

In Figure 6, we present streamlines of the advancing liquid motion in the most interesting case when $D > 1$, i.e., when θ_d, ρ_{1e}^s, A and ρ_{res}^s are sufficiently small. For the curves given in Figure 6 $\theta_s = 20°$, $\theta_d = 30°$, $\rho_{1e}^s = 0.95$, $A = 0.001$, $\rho_{res}^s = 0$, $p_{SG}^s = 0$. Dashed curves are the streamlines of the flow de-

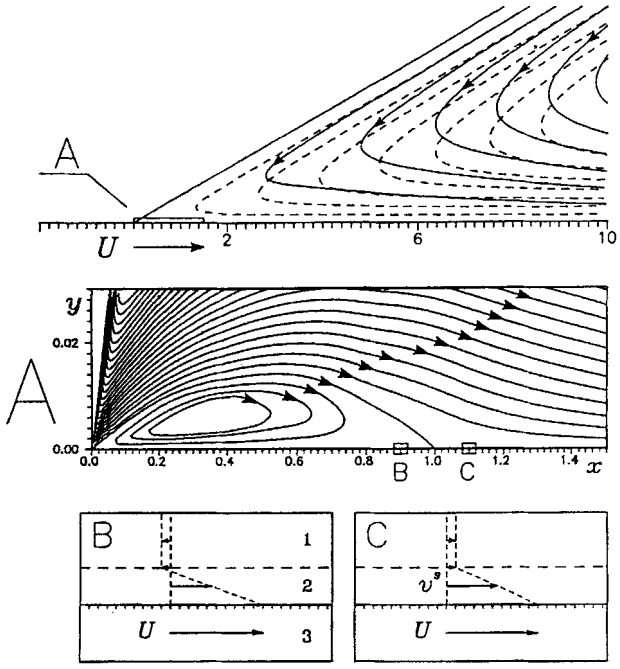

Figure 6. Streamlines for low contact line speeds for $D > 1$ ($\rho^s_{1e} = 0.95$, $\theta_s = 20°$, $\theta_d = 30°$, $A = 0.001$, $\rho^s_{res} = 0$, $\rho^s_{res}(= p^s_{SG}) = 0$).

The region with closed streamlines is present in the vicinity of the contact line (magnified view A). Magnified views B and C show the velocity distribution across the liquid-solid interface. Dashed curves show the streamlines of the classical solution.

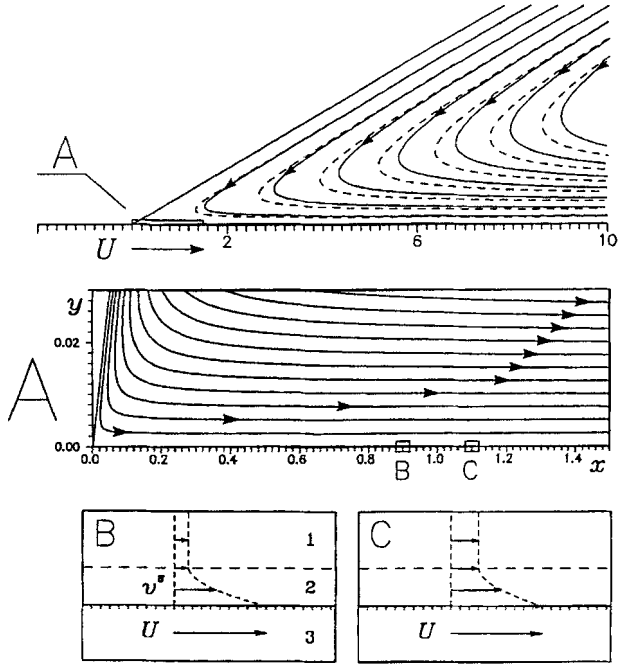

Figure 7. Streamlines for $D < 1$.

$A = 1$ and the values of the other parameters are the same as in Figure 6.

scribed by the classical solution (Eq. 7). Magnified views B and C show the velocity distribution across the liquid-solid interface and in the adjacent liquid.

If $D > 1$, then in the vicinity of the contact line there is a zone with closed streamlines. We use the dimension of this zone to make dimensionless the coordinates in Figure 7 as well. The zone with closed streamlines appears due to the region of reverse slip at the liquid-facing side of the liquid-solid interfacial layer. Reverse slip is caused by the surface pressure gradient along the liquid-solid interface, which increases as $r \to 0$. The hydrodynamic analog of the flow in the interfacial layer is a combination of Couette and Hagen-Poiseuille flows in a plane channel with nonconstant pressure gradient along the channel. It is noteworthy that in our model, everywhere except the contact line itself a *real* slippage does not occur: at the solid-facing side of the liquid-solid interfacial layer the velocity is equal to the velocity of the solid. This fact is in complete agreement with recent results obtained by Koplik et al. (1988) and Thompson and Robbins (1989) by means of a molecular dynamics simulation of the contact line motion. They found that the no-slip boundary condition broke down within ≈ 2 atomic spacing from the contact line, that is, in the three-phase interaction region if this assertion is translated into a thermodynamic language used here.

As the speed of the liquid spreading increases, the dynamic contact angle also increases and the relative slip velocity decreases. Here again we speak about *apparent* slip on the liquid-facing side of the liquid-solid interface. In contrast to slip models (Dussan V., 1979; Shikhmurzaev, 1993a, for review) the flow field tends to that of the classical solution as $\theta_d \to 180°$.

The zone of closed streamlines diminishes as V increases and disappears when D becomes equal to 1. It is interesting that in the advancing contact line motion, an increase of ρ^s_{res} *diminishes* relative slip at the liquid-facing side of the liquid-solid interface: the reverse slip turns into complete and then into partial. This result does not confirm the idea that the precursor film can play the role of a particular kind of a lubricant and lead to apparent slipping of a liquid on a solid boundary: if the film is microscopic, it diminishes the relative degree of apparent slip on a solid; if the film is macroscopic, then it is necessary to consider its edge as the contact line, therefore, simply changing the location of the region of interest.

In the receding contact line motion the zone with closed streamlines also appears as $D > 1$. This condition is strongly influenced by the function $\rho^s_{res}(V)$.

The curves in Figure 7 were obtained for $A = 1$, and the same values of the other parameters as in Figure 6. The region of closed streamlines is absent, though the distribution of v^s_2 along the liquid-solid interface is the same as in Figure 6.

The flow caused by the surface-tension gradient is known in hydrodynamics as the Marangoni effect (Scriven and Sterning, 1960; Napolitano, 1986). In the situations considered in literature, the surface tension gradients appear due to nonhydrodynamic reasons such as temperature and/or surfactant concentration gradients and the dependence of the surface tension on temperature and/or the surfactant concentration. In the case of a moving contact line we are dealing with the effect, which we call the *self-induced* (or *flow-induced*) Marangoni effect, that is the surface-tension gradi-

ent induced by the flow itself and its reverse influence upon the flow.

Discussion

As was shown in the previous sections, the model describes the main experimentally observed macroscopic features of the receding contact line motion listed as (a)–(c) in the second section. A microscopic liquid film present on the solid surface strongly influences the motion (advancing or receding) of the contact line. This film:

- Diminishes the advancing dynamic contact angle and the maximum dynamic contact angle value
- Decreases the rate-of-growth of the advancing contact angle in the case where the static contact angles on prewet and dry solid surfaces are the same
- Increases the maximum speed of liquid displacement from a solid surface
- Diminishes apparent slip on a solid surface.

It is necessary to mention that in general a quantitative comparison of a theory with experiments should take into account the difference between the *measured* and *macroscopic* contact angles; the latter is the contact angle which is used in the free-surface shape determination as a boundary condition for the corresponding hydrodynamic equation. In this article, as well as in some others (Greenspan, 1978; Ehrhard and Davis, 1991; Shikhmurzaev, 1993a, 1994) just the macroscopic contact angle is examined, and the well-known procedure (Cox, 1986) could be applied to determine the deviation of the apparent contact angle from the macroscopic one as the distance from the contact line increases. For high contact line speeds this deviation may be considerable (Ngan and Dussan V., 1982; Dussan V., 1979; Ramé and Garoff, 1991).

Boundary conditions (Eqs. 1–5), which may be considered as a generalization of the Navier boundary condition, are applicable to a number of problems in which the conventional no-slip boundary condition leads to physically unacceptable paradoxes. It should be emphasized that these are paradoxes of the model itself but not of a way in which a particular hydrodynamic problem is simplified (the latter are reviewed, for example, in Goldshtik, 1990). Usually, if the no-slip boundary condition gives rise to a physically unacceptable paradox, slip on the solid surface is introduced, and the paradox is removed. The Navier boundary condition is the most popular among slip models and in some cases, for example, if a purely macroscopic mechanism of the spreading flow over rough surfaces is considered (Hocking, 1976), it has a sound physical background. A slip boundary condition allows us to eliminate shear-stress singularities in many problems especially if the problem involves only liquid-solid boundaries. However, if a slip boundary condition is applied to the moving contact line problem, a number of drawbacks become evident (see Shikhmurzaev, 1993a, 1994, for a discussion). For example, using such boundary conditions, one must *prescribe* the value or the velocity-dependence of the contact angle. In some works it is assumed that the contact angle is equal to the static contact angle even if the contact line is moving. However, as shown in Zhou and Sheng (1990), in this case, if the contact line velocity is sufficiently low, the static and apparent contact angle (the latter was obtained in the framework of different slip theories) are very close to each other, and therefore any measured contact angle should be close to the static contact angle value for these velocities, while experiments show that it is not so. The idea to postulate a velocity-dependence of the contact angle means that an additional adjustable *function*, which must take into account the influence of the contacting material properties, will be introduced in the theory. Obviously, the predicting power of such a theory will be considerably reduced.

Besides this, slip boundary conditions replace the experimentally observed rolling motion of a liquid (Dussan V. and Davis, 1974) by the sliding type (in existing theories $u \sim r^{\lambda}$, $\lambda \geq 1$ as $r \to 0$), and therefore completely change the flow field characteristics.

An essential advantage of the present theory is that it has all the positive features of the Navier boundary condition and eliminates its drawbacks being applied to the moving contact line problem. It is clear that the model holds the rolling character of the liquid motion (see condition 12) and gives the velocity-dependence of the contact angle. It is noteworthy that boundary conditions (Eqs. 1–6) can be easily generalized for the case of an interface between immiscible viscous fluids (Shikhmurzaev, 1993b) so that the splitting of the free interface at the moving contact line is described.

Thus, the developed approach gives a unified regular way of considering different problems where the standard conditions for the Navier-Stokes equations give rise to physically unacceptable situations.

Notation

Ca = capillary number
F = total drag force
$l = U\tau$
p = pressure
p^s = surface pressure (negative surface tension)
p^s_{res} = tangential force per unit length of the contact line on a prewet solid surface
p^s_{SG} = tangential force per unit length of the contact line on a dry solid surface
r = coordinate radius
r_0 = coordinate of the stagnation point
u_r, u_θ = components of the velocity in the polar coordinate system
U_0 = maximum speed of drying
V = dimensionless contact line speed
W = constant

Greek letters

γ = constant
$\epsilon = U\tau/L$
θ_s = static contact angle on a dry solid surface
θ_0 = static contact angle on a prewet solid surface
$\lambda = \gamma\rho^s_0/\sigma$
ρ^s = surface density
ρ^s_0 = surface density corresponding to zero surface pressure
ρ^s_r = constant
ρ^s_{res} = surface density of the microscopic residual film
σ = equilibrium surface tension
ψ = stream function
$\psi_{(0)}$ = stream function of the outer solution

Literature Cited

Ablett, R., "An Investigation of the Angle of Contact between Paraffin Wax and Water," *Philos. Mag.*, **46**, 244 (1923).

Ausserré, D., A. M. Picard, and L. Léger, "Existence and Role of the Precursor Film in the Spreading of Polymer Liquids," *Phys. Rev. Lett.*, **57**, 2671 (1986).

Bartell, F. E., and A. D. Wooley, "Solid-Liquid-Air Contact Angles and their Dependence upon the Surface Condition of the Solid," *J. Amer. Chem. Soc.*, **55**, 3518 (1933).
Bedeaux, D., A. M. Albano, and P. Mazur, "Boundary Conditions and Non-Equilibrium Thermodynamics," *Physica*, **A82**, 438 (1976).
Blake, T. D., "Dynamic Contact Angles and Wetting Kinetics," *Wettability*, J. C. Berg, ed., Marcel Dekker, New York (1993).
Blake, T. D., and K. J. Ruschak, "A Maximum Speed of Wetting," *Nature* (London), **282**, 489 (1979).
Bolton, B., and S. Middleman, "Air Entrainment in a Roll Coating System," *Chem. Eng. Sci.*, **35**, 597 (1980).
Bretherton, F. P., "The Motion of Long Bubbles in Tubes," *J. Fluid Mech.*, **10**, 166 (1961).
Churaev, N. V., V. D. Sobolev, and A. N. Somov, "Slippage of Liquids over Lyophobic Solid Surfaces," *J. Colloid Interf. Sci.*, **97**, 574 (1984).
Cox, R. G., "The Spreading of a Liquid on a Rough Solid Surface," *J. Fluid Mech.*, **131**, 1 (1983).
Cox, R. G., "The Dynamics of the Spreading of Liquids on a Solid Surface. Part 1. Viscous Flow," *J. Fluid Mech.*, **168**, 169 (1986).
Davies, B., and B. Martin, "Numerical Inversion of the Laplace Transform: a Survey and Comparison Methods," *J. Comput. Phys.*, **33**, 1 (1979).
Dussan V., E. B., "On the Spreading of Liquids on Solid Surfaces: Static and Dynamic Contact Lines," *Ann. Rev. Fluid Mech.*, **11**, 371 (1979).
Dussan V., E. B., and S. H. Davis, "On the Motion of a Fluid-Fluid Interface along a Solid Surface," *J. Fluid Mech.*, **65**, 71 (1974).
Dussan V., E. B., E. Ramé, and S. Garoff, "On Identifying the Appropriate Boundary Conditions at a Moving Contact Line: an Experimental Investigation," *J. Fluid Mech.*, **230**, 97 (1991).
Ehrhard, P., and S. H. Davis, "Non-Isothermal Spreading of Liquid Drops on Horizontal Plates," *J. Fluid Mech.*, **229**, 365 (1991).
Elliott, G. E. P., and A. C. Riddiford, "Dynamic Contact Angles: I. The Effect of Impressed Motion," *J. Colloid Interf. Sci.*, **23**, 389 (1967).
Fowkes, F. M., "Attractive Forces at Solid-Liquid Interfaces," *Wetting*, Vol. 25, Soc. of Chem. Ind., London, p. 3 (1967).
de Gennes, P. G., "Wetting: Statics and Dynamics," *Rev. Mod. Phys.*, **57**, 827 (1985).
Ghannam, M. T., and M. N. Esmail, "The Effect of Pre-Wetting on Dynamic Contact Angles," *Can. J. Chem. Eng.*, **70**, 408 (1992).
Gibbs, J. W., *The Scientific Papers of Gibbs*, Vol. 1, Dover, New York (1961).
Goldshtik, M. A., "Viscous-Flow Paradoxes," *Ann. Rev. Fluid Mech.*, **22**, 441 (1990).
Greenspan, H. P., "On the Motion of a Small Viscous Droplet that Wets a Surface," *J. Fluid Mech.*, **84**, Part 1, 125 (1978).
Hansen, R. S., and M. Miotto, "Relaxation Phenomena and Contact Angle Hysteresis," *J. Amer. Chem. Soc.*, **79**, 1765 (1957).
Hocking, L. M., "A Moving Fluid Interface on a Rough Surface," *J. Fluid Mech.*, **76**, Part 4, 801 (1976).
Hocking, L. M., "A Moving Fluid Interface. Part 2. The Removal of the Force Singularity by a Slip Flow," *J. Fluid Mech.*, **79**, Part 2, 209 (1977).
Hopf, W., and H. Stechemesser, "Three-Phase Contact Line Movement in Systems with and without Surfactant," *Colloid Surf.*, **33**, 25 (1988).
Inverarity, G., "Dynamic Wetting of Glass Fibre and Polymer Fibre," *Br. Polym. J.*, **1**, 245 (1969).
Joanny, J. F., and P. G. de Gennes, "A Model for Contact Angle Hysteresis," *J. Chem. Phys.*, **81**, 552 (1984).
Johnson, R. E., R. H. Dettre, and D. A. Brandreth, "Dynamic Contact Angles and Contact Angle Hysteresis," *J. Colloid Interf. Sci.*, **62**, 205 (1977).
Kochurova, N. N., Yu. A. Shvechenkov, and A. I. Rusanov, "Determination of the Surface Tension of Water by the Oscillating Jet Method," *Colloid J.* (USSR), **36**, 785 (1974).
Koplik, J., J. R. Banavar, and J. F. Willemsen, "Molecular Dynamics of Poiseuille Flow and Moving Contact Lines," *Phys. Rev. Lett.*, **60**, 1282 (1988).
Landau, L. D., and V. G. Levich, "Dragging of a Liquid by a Moving Plate," *Acta Physicochim. USSR*, **17**, 42 (1942).
Moffatt, H. K., "Viscous and Resistive Eddies Near a Sharp Corner," *J. Fluid Mech.*, **18**, Part 1, 1 (1964).
Napolitano, L. G., "Recent Development of Marangoni Flows Theory and Experimental Results," *Adv. Spac. Res.*, **6**(5), 19 (1986).
Ngan, C. G., and E. B. Dussan V., "On the Nature of the Dynamic Contact Angle: an Experimental Study," *J. Fluid Mech.*, **118**, 27 (1982).
Novotny, V. J., and A. Marmur, "Wetting Autophobisity," *J. Colloid Interf. Sci.* **145**, 355 (1991).
Oliver, J. F., and S. G. Mason, "Microspreading Studies on Rough Surfaces by Scanning Electron Microscopy," *J. Colloid Interf. Sci.*, **60**, 480 (1977).
Pomeau, Y., and J. Vannimenus, "Contact Angle on Heterogeneous Surface: Weak Heterogeneity," *J. Colloid Interf. Sci.*, **104**, 477 (1985).
Rillaerts, E., and P. Joos, "The Dynamic Contact Angle," *Chem. Eng. Sci.*, **35**, 883 (1980).
Rose, W., and R. W. Heins, "Moving Interfaces and Contact Angle Rate Dependence," *J. Colloid Interf. Sci.*, **17**, 39 (1962).
Rowlinson, J. S., and B. Widom, *Molecular Theory of Capillarity*, Clarendon, Oxford (1982).
Scriven, L. E., and C. V. Sterning, "The Marangoni Effects," *Nature*, **187**, 186 (1960).
Sedev, R. V., and J. G. Petrov, "Influence of Geometry on Steady Dewetting Kinetics," *Colloid Surf.*, **62**, 141 (1992).
Shikhmurzaev, Y. D., "Hydrodynamics of Wetting: The Displacement of a Gas by a Liquid from a Solid Surface," *All-Union Cong. on Theor. and Appl. Mech.*, Moscow (Aug. 15–21, 1991).
Shikhmurzaev, Y. D., "The Moving Contact Line on a Smooth Solid Surface," *Int. J. Multiphase Flow*, **19**, 589 (1993a).
Shikhmurzaev, Y. D., "A Two-Layer Model of an Interface between Immiscible Fluids," *Physica*, **A192**, 47 (1993b).
Shikhmurzaev, Y. D., "Mathematical Modeling of Wetting Hydrodynamics," *Fluid Dyn. Res.*, **13**, 45 (1994).
Teletzke, G. F., "Thin Liquid Films: Molecular Theory and Hydrodynamic Implications," PhD Thesis, Univ. Minnesota, Minneapolis (1983).
Teletzke, K., H. T. Davis, and L. E. Scriven, "Wetting Hydrodynamics," *Revue Phys. Appl.*, **23**, 989 (1988).
Templeton, C. C., "A Study of Displacements in Microscopic Capillaries," *Trans. AIME*, **201**, 162 (1954).
Templeton, C. C., "Oil-Water Displacements in Microscopic Capillaries," *Trans. AIME*, **207**, 211 (1956).
Thompson, P. A., and M. O. Robbins, "Simulation of Contact-Line Motion: Slip and the Dynamic Contact Angle," *Phys. Rev. Lett.*, **63**, 766 (1989).
Vaillant, M. P., "Sur un Precédé de Mesure des Grandes Résistances Polarisables et son Application a la Mesure de la Résistance de Liquides," *C. R. Acad. Sci. Paris*, **156**, 307 (1913).
Wilkinson, W., "Entrainment of Air by a Solid Surface Entering a Liquid/Air Interface," *Chem. Eng. Sci.*, **30**, 1227 (1975).
Yarnold, G. D., "The Motion of a Mercury Index in a Capillary Tube," *Proc. Phys. Soc.*, **50**, 540 (1938).
Zhou, M. Y., and P. Sheng, "Dynamics of Immiscible Fluid Displacement in a Capillary Tube," *Phys. Rev. Lett.*, **64**, 882 (1990).

Manuscript received Oct. 24, 1994, and revision received May 15, 1995.